

Nanoscale Methods for Single-Molecule Electrochemistry

Klaus Mathwig,¹ Thijs J. Aartsma,²
Gerard W. Canters,² and Serge G. Lemay¹

¹MESA+ Institute for Nanotechnology, University of Twente, 7500 AE Enschede, the Netherlands; email: k.h.mathwig@utwente.nl, s.g.lemay@utwente.nl

²Leiden Institute of Physics, Huygens Laboratory, Leiden University, 2333 CA Leiden, the Netherlands; email: aartsma@physics.leidenuniv.nl, canters@chem.leidenuniv.nl

Annu. Rev. Anal. Chem. 2014. 7:383–404

First published online as a Review in Advance on June 9, 2014

The *Annual Review of Analytical Chemistry* is online at anchem.annualreviews.org

This article's doi:
10.1146/annurev-anchem-062012-092557

Copyright © 2014 by Annual Reviews.
All rights reserved

Keywords

electron transfer, fluorescence detection, metal-molecule-metal junctions, electrochemical nanofluidics

Abstract

The development of experiments capable of probing individual molecules has led to major breakthroughs in fields ranging from molecular electronics to biophysics, allowing direct tests of knowledge derived from macroscopic measurements and enabling new assays that probe population heterogeneities and internal molecular dynamics. Although still somewhat in their infancy, such methods are also being developed for probing molecular systems in solution using electrochemical transduction mechanisms. Here we outline the present status of this emerging field, concentrating in particular on optical methods, metal-molecule-metal junctions, and electrochemical nanofluidic devices.

INTRODUCTION

From a phenomenological perspective, electrochemistry is dominated by macroscopic concepts such as concentrations and average fluxes: The underlying molecular structure enters our formalisms mostly via its influence on bulk constants such as electron transfer (ET) rates. Nevertheless, the rapid development of nanometer-scale probes renders electrochemical assays near or at the level of single molecules an increasingly accessible reality.

Why would one be interested in performing single-molecule electrochemistry? To answer this question, it is interesting to chart the progression of single-molecule techniques in other subfields where a relatively mature “single-molecule toolkit” has evolved (1). This toolkit spans a broad range of methods based on mechanical (atomic force microscopy, optical tweezers), electrical [scanning tunneling microscopy (STM), ion channels], or optical (fluorescence) transduction mechanisms. Typically starting as a *tour de force* experiment in which its basic principles are established, a new method is then applied to progressively more complex systems and questions. Early experiments are often motivated by the method itself: How does one relate the molecular-level observations to known bulk behavior? This exercise can serve as a powerful pedagogical tool, as illustrated by a recent study of the mass-action law (2). The new single-molecule technique is then subject to questions that inherently require this type of scrutiny, such as systems in which the number of molecules of interest is small, in which the spatial localization of individual molecules is critical, or in which a population of nominally identical molecules is in fact heterogeneous due to defects or the ability to adopt different internal states. It will also be expected to unveil the internal processes and dynamics of a single (macro)molecule. In a final stage, single-molecule measurements can also become the enablers of new analytical methods that take advantage of their supreme sensitivity and real-time capabilities. A striking illustration is third-generation DNA sequencing methods, which rely on tracking the activity of a single DNA polymerase enzyme using fluorescence (3). Against this backdrop, it is fair to say that many aspects of single-molecule electrochemistry are still in the early stages of method development, validation, and rationalization. Whether new tools based on electrochemistry are as successful as other established methods, either alone or as complements to other techniques, remains to be seen. It is our belief that this question cannot be definitively answered until the methods become sufficiently well developed to provide the basis for a realistic evaluation of their capabilities and limitations.

DEFINING SINGLE-MOLECULE ELECTROCHEMISTRY

The term single-molecule electrochemistry spans a broad range of concepts and experiments. We concentrate here solely on situations in which electron-transfer reactions play a central role. We further confine ourselves to systems in solution at or near room temperature. Even within this relatively narrow definition, the term single-molecule electrochemistry already describes three broad scenarios:

1. Monitoring the redox state of a single molecule: This can be achieved by using fluorescence techniques or by addressing individual molecules in a metal-molecule-metal junction.
2. Detecting the charge transferred as a single molecule is reduced and/or oxidized: In practice it has so far proven impossible to detect the few electron(s) transferred during a single oxidation or reduction event by virtue of the amount of charge being too small for accurate detection at room temperature. Such measurements therefore necessarily average over several successive reduction/oxidation cycles so as to generate enough charge to allow detection.
3. Monitoring the electrocatalytic current from a single molecule: Here the catalytic process provides inherent amplification, a single catalyst providing a continuous stream of

electron-transfer events leading to a measurable current. This approach has recently been applied successfully to nanoscale catalysts such as individual metal nanoparticles (4–8), but not to individual molecules. For example, attempts at detecting the catalytic current from a few macromolecules via downscaling of the protein-film-voltammetry approach (9, 10) can currently achieve a resolution of only ~ 50 molecules (11). For this reason we do not discuss this approach further.

OPTICAL METHODS

One way out of the single-molecule-sensitivity dilemma is the transformation of the electrochemical events to the optical domain. In recent years, the use of fluorescence-based techniques for this purpose has been explored. When the fluorescence intensity varies with the redox state of the compound to be studied, an appreciable gain in the signal-to-noise ratio can be achieved. With a typical fluorescence lifetime of 10 ns and redox events occurring at a rate of 100 s^{-1} , 10^5 to 10^7 photons per redox event can be recorded, depending on optical saturation and fluorescence quantum yield. Moreover, the much higher energy content of a photon at a wavelength of, say, 400 nm compared to that of an electrochemically driven event allows for improved detection efficiency. For the transformation of the electrochemical to the optical domain, various strategies have been attempted. The field remains in its infancy, and the prospects of each technique still have to be assessed in practice. The following approaches have been explored in recent years and are reviewed briefly here:

1. Use of fluorescent molecules: The molecule of interest is fluorescent by itself. The fluorescence intensity varies with the redox state of the compound.
2. Chemiluminescence: Redox events become visible by chemiluminescence.
3. Fluorescent labeling: The compound to be investigated is fluorescently labeled.
4. Surface enhanced resonance Raman spectroscopy: SERS distinguishes between different redox states.
5. Electrocatalysis: This is used to produce fluorescent products.

Fluorescent Molecules

When the fluorescence intensity of an electrochemically active compound varies with its redox state, its electrochemical response can be studied by monitoring fluorescence intensity (12; see also sidebar, Blinking). One of the first examples to be reported dealt with the study of cresyl violet in solution by confocal microscopy while the solution was subjected to cyclic voltammetry

BLINKING

Studying redox events at the single-molecule level by monitoring fluorescence intensity or lifetime is often hampered by the phenomenon of blinking. Blinking is caused by nonfluorescent decay of the excited single molecule to the triplet state or its photochemical (reversible) transformation into a positively or negatively charged radical ion. Photochemical transformation may eventually also result in the complete loss of fluorescence, hence the continuing quest for fluorophores in which blinking, bleaching, or both are reduced to a minimum. A recent development aims at protecting the fluorophore by surrounding it with a shell of a dendritic polymer. Such a new probe may have special use in biological imaging (15).

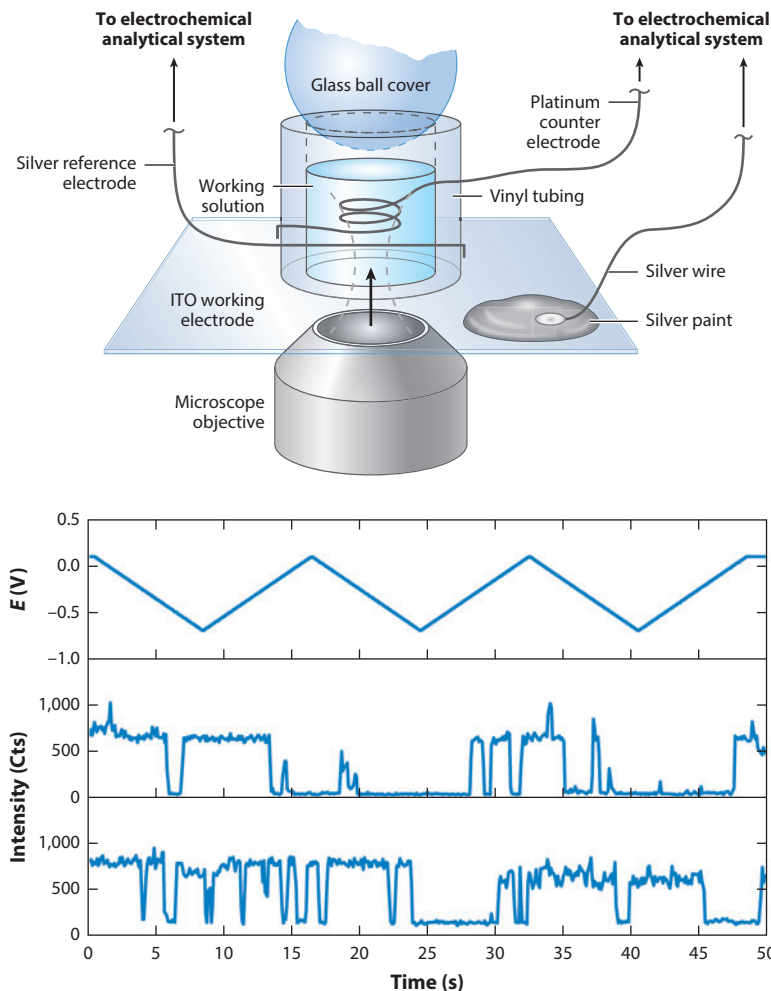


Figure 1

(*top*) Schematic of a conventional electrochemical cell coupled with scanning confocal fluorescence microscopy. A potentiostat was connected to the cell equipped with a three-electrode system using a transparent indium tin oxide (ITO)/glass cover slip as the working electrode. Adapted from Reference 13, with permission of the Royal Society of Chemistry. (*bottom*) The top panel shows a plot of the voltage E (V) versus time used in cyclic voltammetry. The below panels are plots of the fluorescence intensity versus time of two single cresyl violet molecules adsorbed on sodium montmorillonite/ITO during cyclic voltammetry scans. From Reference 14, Copyright © (2009) by American Chemical Society.

(CV; see **Figure 1**, top panel) (13). By choosing the cresyl violet concentration low enough, the confocal volume of the microscope was traversed by one molecule at a time, and the redox state of each molecule could be determined from the observed fluorescence intensity. From their observations, the authors could show—on a single-molecule level—that reduced cresyl violet molecules fluoresce strongly when oxidized, but not at all when reduced. In a second attempt to combine single-molecule spectroscopy with electrochemical control, the authors immobilized cresyl violet on transparent indium tin oxide (ITO) electrodes covered with transparent montmorillonite nanoparticles (14). In this experiment, fluorescent time traces of single immobilized particles could

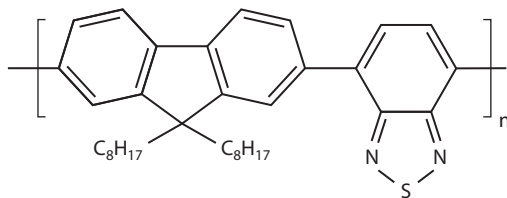


Figure 2

F8BT, a molecule that may find application in devices such as photovoltaic cells and light-emitting diodes.

be observed while scanning the potential (see **Figure 1**, bottom panel). The analysis and interpretation of the data were hampered by the frequent blinking of the cresyl violet, but the average off and on times of the particles on the electrode could be established and proved to be in line with the ensemble-measured ET rates.

A recent study employs a device in which small 60–150-nm-wide holes are created by means of focused ion beam technology in a 100-nm-thick gold working electrode (16). The holes function as zero-mode waveguides (ZMWs). In a four-step chemical process, flavin adenine dinucleotide (FAD) was immobilized on the walls of the nanopores. By a judicious choice of the FAD concentration employed during the immobilization procedure, the ZMW holes contain mostly just one molecule of FAD. These could now be addressed individually in a classical three-electrode CV setup. The FAD fluorescence, which is strong with FAD in the oxidized form and absent with FAD in the reduced form, could be studied as a function of the applied electrical potential. Analysis of fluorescence time traces of individual ZMWs demonstrated the occurrence of a spread in midpoint potentials and ET rates (16).

In materials science, the application of fluorescent single-molecule techniques has led to important new insights. Bard, Barbara, and coworkers (17, 18) prepared polymerized 9,9-dioctylfluorene-cobenzothiadiazole (F8BT; see **Figure 2**) molecules in polystyrene particles, which were immobilized on an ITO surface. F8BT luminescence occurs in the 500–700-nm range but the emission is quenched upon oxidation (hole injection). Wide-field images of the ITO surface under 488-nm illumination exhibited bright spots, each corresponding to a single polymerized F8BT molecule. In combination with a three-electrode setup, the electrochemical behavior of the single molecules could be studied. Hole creation appeared partly irreversible due to conversion of the holes into deep (permanent) traps. The development in time of the holes/traps, the recovery in time, and the half-wave distributions for the fluorescence quenching could be determined.

Zhang et al. (19) spin coated 1,10-dioctadecyl-3,3,30,30-tetramethylindole-dicyanin (DiD) dye molecules on glass and covered them with an ITO layer upon which a poly(methyl methacrylate) (PMMA: $M_w = 15,000$; $T_g = 82.1^\circ\text{C}$) film was deposited. By sending an external electric current through the ITO layer, forward and backward ET between the ITO and ground and excited state DiD molecules were promoted, leading to quenching of the DiD fluorescence. The fluorescence of individual DiD molecules was observed as a function of the applied current, and information was obtained about the various rates of ET between the ITO and the DiD molecules.

Electrogenerated Chemiluminescence

There has been one example reported so far in which chemiluminescence is used as a tool to follow the electrochemical activity of immobilized redox-active molecules, i.e., F8BT (20). Polymerized F8BT was deposited on an ITO working electrode in the form of nanoparticles. When oxidized

electrochemically, the oxidized F8BT may react with tri-*n*-propylamine, which is present in the solution phase. This gives rise to photoexcitation and subsequent fluorescence of the nanoparticle. So far, the ensemble averaged response on a change in the applied potential of a three-electrode electrochemical cell can be measured; however, extending this to the single particle level has yet to be realized.

Fluorescent Labeling of Redox Proteins

Interestingly, the first report on fluorescently detected electrochemistry was not based on studies of simple organic or inorganic molecules but, rather, of proteins. Oxidoreductases often contain cofactors whose absorption spectra depend on their redox states. A fluorescent label attached to the protein, when excited, may transfer part of its excited state energy to the cofactor by means of Förster resonant energy transfer (FRET). The redox cofactor is usually nonfluorescent. The label fluorescence will therefore be (partly) quenched depending on the label versus cofactor distance and on the spectral overlap between label fluorescence and cofactor absorption. When the absorption spectrum of the cofactor varies, the observed fluorescence will vary, too.

The principle was neatly illustrated on azurin, a protein isolated from *Pseudomonas aeruginosa*. The protein fulfills the role of electron carrier, most likely within the oxidative stress response of the organism (21), and has a Cu ion in its active site. The Cu may occur in the reduced (Cu^{1+}) and the oxidized (Cu^{2+}) state between which it switches during ET. In the reduced state, the protein is colorless; in the oxidized form, it is dark blue as a result of a π - π^* transition involving the Cu ion. The fluorescence of an attached Cy5 label was found to clearly reflect the oxidation state of the protein (22, 23). In subsequent studies, it was shown how the principle can be applied to study enzyme kinetics at the single-molecule level (24–26).

It proved possible to combine this technique with electrochemical measurements (see **Figure 3**). Fluorescently labeled azurin molecules were immobilized on a transparent gold electrode covered by a self-assembled monolayer (SAM) of 1-hexanethiol. Scanning the potential by CV in a three-electrode electrochemical cell clearly showed that the variation in fluorescence ran in parallel with the potential; the current variation was too small to be detectable. Initially, the signals from regions of interest (ROIs) on the electrode surface contained a relatively large number of molecules ($\geq 1,000$) (27). In a later attempt, the ROIs could be confined to approximately 100 molecules (28). The observed spread in midpoint potential of individual molecules amounted to roughly 100 mV, and the spread in the heterogeneous ET rate was considerable (from 0.3 to 60 s^{-1}) (see **Figure 4**). Patil & Davis (29) later showed that the dispersion of the electrochemical parameters depended on the crystallinity of the SAM applied to the Au electrode on which the azurin was immobilized. The higher the crystallinity, the smaller the spread (29).

Surface-Enhanced Resonance Raman Spectroscopy

Although Raman spectroscopy is based on the analysis of scattered light as opposed to fluorescent light, the method is considered here because as a light-based technique, it can be applied to the detection and study of the redox events of single molecules. Single molecules can be observed with surface-enhanced Raman scattering using a roughened Ag surface. The sharp features of the Ag surface induce enhanced excitation and scattering cross sections of an immobilized molecule that more than compensate the quenching exerted by the nearby conducting electrons of the silver. A necessary and sufficient condition for observing the resonantly enhanced features of a single molecule is that when resonant excitation is applied, the electronic transition shifts out of resonance when the redox state of the molecule changes, or, alternatively, the Raman

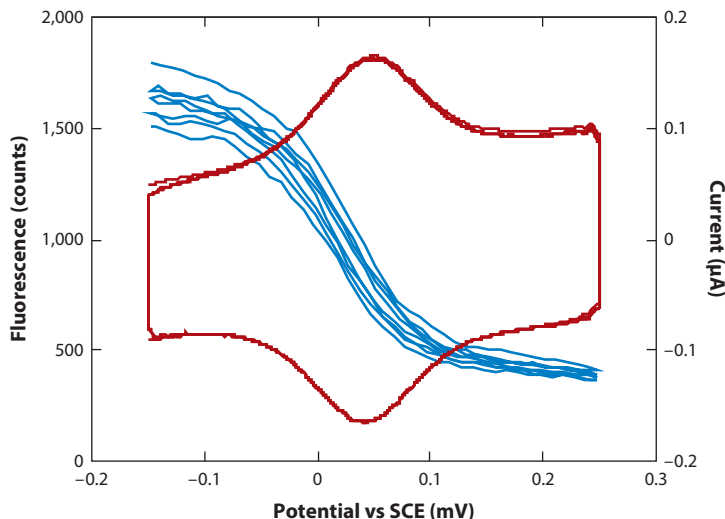


Figure 3

The red line is the current-detected cyclic voltammogram of a monolayer of azurin on a flat gold electrode. The blue lines are cyclic voltammograms detected by epifluorescent microscopy of Cy5-labeled, wild-type azurin at a 100-mV s^{-1} scan rate. The fluorescence curve reflects the change in the redox state of the labeled azurin as a function of potential. Each fluorescence trace represents the response of a $300 \times 300\text{-nm}$ area (the diffraction-limited resolution of the microscope) of the fluorescence image of the sample. The detection limit was estimated to be approximately 100 molecules. From Reference 28, Copyright © 2010 WILEY-VCH Verlag GmbH & Co. KGaA, Weinheim.

spectrum must exhibit redox-state-sensitive vibrational transitions when nonresonant excitation is applied.

Cortés et al.'s (30) study provides an example of the former method. They immobilized Nile blue (NB) and Rhodamine 6G (Rh6G) on Ag colloidal particles by co-deposition on a Ag electrode. To vary the redox state of the dyes, a three-electrode electrochemical cell was employed. At 633-nm excitation, oxidized NB is resonantly excited and exhibits a characteristic Raman mode at 590 cm^{-1} . When NB is reduced, the absorption disappears and thereby the Raman spectrum. For calibration purposes, the Rh6G mode at 610 cm^{-1} , which is almost unperturbed when the potential is cycled, was used. The response of a single NB molecule upon cycling the potential is clear and provides an indirect amplification of single-molecule electrochemistry events that can be observed with high specificity. Extension of the technique to *in vivo* and biologically relevant experiments is foreseen (see sidebar, *In Vivo Imaging*).

The second approach is exemplified by the work of Wang et al. (33), who immobilized hemin molecules on Ag nanoparticles and used poly-L-lysine to deposit the particles on a glass cover slip. Confocal spectroscopy was used to study the Raman spectra of individual hemin molecules. Two vibrational modes were used as diagnostics for the redox and spin state of the hemin. Ground-state fluctuations of these modes appeared indicative of the electron exchange (back and forth) between Ag and hemin. These fluctuations were further investigated by spectroelectrochemistry, in which the Ag particles were deposited on an ITO layer applied to a cover slip. The effect on the ET rate of applying a potential difference in a three-electrode setup in which the ITO electrode served as the working electrode could be investigated. It was found that the ET between Ag particles and hemin in the ground state is driven primarily by thermal fluctuations.

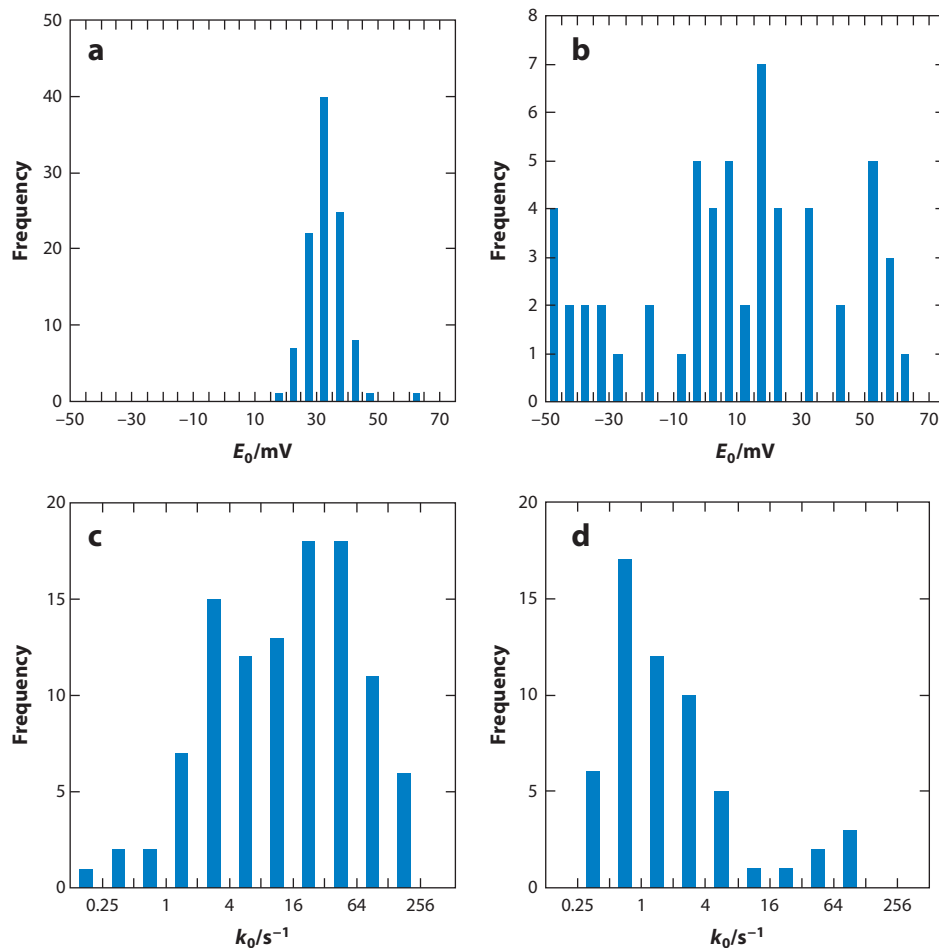


Figure 4

Data obtained from all fluorescence-detected cyclic voltammograms (FCVs) of a full monolayer of protein [using (a,c) epifluorescence detection] and of a dilute submonolayer [using (b,d) total internal reflection-excited fluorescence (TIRF)]. (a) Histogram of midpoint potential values, E_0 , of FCVs of randomly selected regions of interest (ROIs), showing a 14-mV spread [full width half maximum (FWHM)] around an average of 28 mV. Bin values on the x-axis refer to the upper limit of the bin range for all histograms shown. (b) Histogram of midpoint potential values, E_0 , obtained from all TIRF ROI FCV curves showing a 70-mV spread (FWHM) around an average of 16 mV. (c) Histogram of standard electron-transfer rate constants, k_0 , obtained from all epifluorescence ROI FCV curves showing values ranging from 0.1 s^{-1} to 200 s^{-1} . (d) Histogram of standard electron-transfer rate constants, k_0 , obtained from all TIRF ROI FCV curves showing values clustering between 0.5 and 2 s^{-1} with a high- k_0 tail up to 100 s^{-1} . From Reference 28, Copyright © 2010 WILEY-VCH Verlag GmbH & Co. KGaA, Weinheim.

Electrocatalysis Produces Fluorescent Products

An interesting application of single-molecule spectroelectrochemistry is provided by the work of Peng Chen and coworkers (34) on the catalytic activity of carbon nanotubes. Single-walled carbon nanotubes (SWNTs) can catalyze the electrochemical reduction of the nonfluorescent resazurin to the fluorescent resorufin and the subsequent reduction of resorufin to the nonfluorescent

IN VIVO IMAGING

The application of single-molecule fluorescence techniques is rapidly gaining ground in *in vivo* bioimaging studies. By “decorating” cellular and subcellular structures with blinking fluorophores, flashes of light stochastically distributed in time can be observed with high resolution. Afterward, the flashes can be composed into a full picture of the object studied. Ideally, the blinking behavior of the fluorophore should be under control of the experimenter. (For an instructive review on this topic, see Reference 31). A closely related topic deals with the imaging of reactive oxygen and nitrogen species in the cell. Special probes are being developed that are based on semiconducting polymer nanoparticles. Their unusual brightness, especially, offers new perspectives for *in vivo* imaging (32).

dihydroresorufin. The three states are connected in a cyclic reaction scheme that was investigated by immobilizing the SWNTs on an ITO-covered glass slide. The ITO layer served, again, as the working electrode in a three-electrode electrochemical cell. Single reaction sites on the SWNTs could be observed under confocal microscopy, and the dispersion in reaction rates or heterogeneity in the active sites on the SWNTs could be mapped out.

MOLECULAR JUNCTIONS

An alternative detection modality to optical measurements is to directly detect the charge transferred in electrochemical processes. From an experimental point of view, directly measuring ET at the molecular scale suffers from several drawbacks:

1. The resolution of electronic measurements is limited to an energy spread of $\sim 3.5 k_B T$, or ~ 90 mV for a single-electron process at room temperature (35). This is extremely poor compared to the energy (i.e., color) discrimination of optical methods.
2. A low optical signal can be more readily detected: Using electron-multiplied charge-coupled device (CCD) sensors, avalanche photodiodes, or photomultiplier tubes, single photons can be detected routinely with high time resolution and at high acquisition rates. Moreover, CCD sensor arrays allow spatially resolved imaging. In contrast, it is in practice impossible to detect a single electron in liquid at room temperature due to the parasitic instrumental noise introduced by the amplifier circuit.
3. As a result, electrical detection necessarily requires averaging over several redox events.

However, all-electrical sensing also has advantages compared to optical detection, and both measurement schemes can thus be complementary:

1. Not all redox analytes are optically active or can be coupled to an optically active mediator.
2. The wide range of voltammetric and amperometric methods available in direct electrochemical measurements is well suited for exploratory studies.
3. Due to the absence of optical elements in all-electrical detection, the formidable advances in microfabrication technology of the past decades can be directly harnessed. Complex assays can thus be miniaturized, combined in massively parallel configurations, integrated with other fluidic components, and mass-produced at relatively low cost.
4. Consequently, the integration of nanoscale assays in lab-on-a-chip applications, even at the scale of consumer products, becomes conceivable.

Conceptually, perhaps the most straightforward way to electrically address a single molecule is to anchor it between electrodes so as to create a metal-molecule-metal junction, as illustrated in **Figure 5a** (see also sidebar, Molecular Junctions as Transistors). A potential difference ΔU is

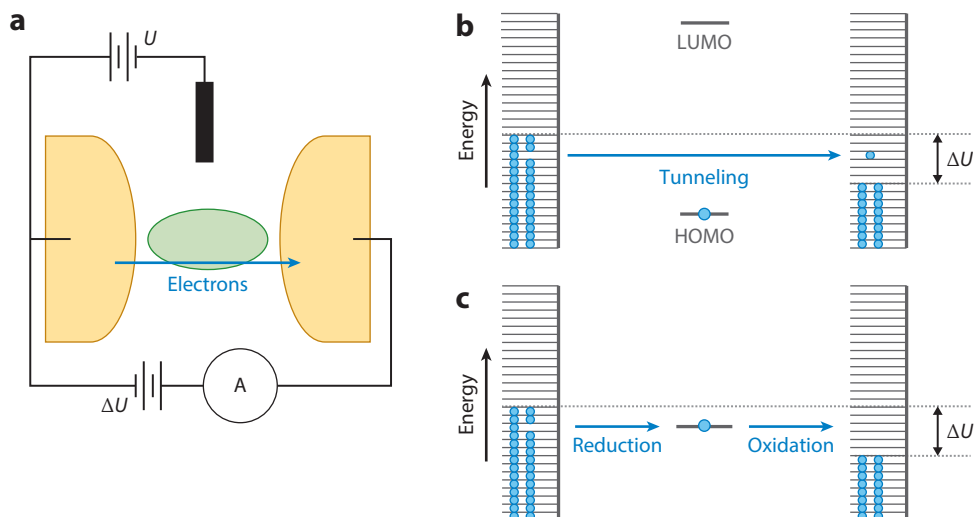


Figure 5

Molecular junctions. (a) Sketch of the experimental configuration. A redox molecule (*green*) acts as a bridge between two electrodes (*yellow*), facilitating electron tunneling. A potential ΔU is applied between the electrodes while the reference potential of the electrolyte is independently controlled via a reference electrode (potential U). (b) Electron energy diagram for the direct tunneling mechanism, in which electrons tunnel between occupied states of one electrode and unoccupied states of the other. The blue dots represent occupied energy levels. The occupations of the bridge molecule's HOMO and LUMO energy levels remain unchanged during this process. (c) Corresponding diagram for the sequential tunneling mechanism. The electrodes are biased such that the first electrode reduces the bridging molecule while the second oxidizes it. This causes a reduction/oxidation cycle, the bridge molecule oscillating between two redox states. Abbreviations: HOMO, highest occupied molecular orbital; LUMO, lowest unoccupied molecular orbital.

applied between the two electrodes that can generate an electrical current through the molecule. This current acts as a probe of the molecule's redox state, which can in turn be controlled by independently adjusting the potential of the surrounding electrolyte via a reference electrode immersed in the solution (as signified by the potential U in **Figure 5a**).

Experimentally, a wide array of techniques has been developed to create the geometry of **Figure 5a**. These include in particular STM (37–43) and atomic force microscopy (44), in which a movable metal tip and a conducting substrate play the role of electrodes; pairs of electrodes separated by only a few nanometers (45, 46); and mechanical break junctions, in which the separation between the electrodes can be controlled (47). Although the basic experimental configuration of **Figure 5a** is essentially conserved across these experiments, several conceptually distinct

MOLECULAR JUNCTIONS AS TRANSISTORS

The configuration of **Figure 5a** exhibits the basic operation of a field-effect transistor, in which the current flowing between source and drain electrodes is modulated via a third electrode, the gate. Indeed, the links between electrochemistry and molecular electronics have been an important driving force for the development of single-molecule junctions (36).

mechanisms may in fact be responsible for observed single-molecule signals. This leads to a correspondingly diverse and complex phenomenology. Both the theory and the experimental status of molecular junction systems were meticulously reviewed by Zhang et al. (48). Although additional experimental and theoretical advances have taken place since, addressing these in detail would take us far beyond the scope of the present review. We therefore limit ourselves to highlighting key aspects of the early experiments and refer the interested reader to more specialized reviews (48–53).

An important class of transduction mechanisms in molecular junctions is direct tunneling, as illustrated in **Figure 5b**. Here electrons tunnel directly between the two electrodes without residing in a long-lived electronic state of the intervening molecule. This occurs via the so-called superexchange mechanism and is usually dominant for situations where the HOMO and the LUMO of the bridge molecule have energies far from the Fermi level of the metal contacts. The magnitude of the tunneling current per molecule is readily measurable (pA–nA for short bridge molecules), rendering single-molecule measurements possible. The bridge molecule does not have to be redox active for such tunneling to take place. If it is, however, the observed tunneling current can differ for different redox states of the molecule; the tunneling current then becomes a probe of the redox state.

A second transduction mechanism develops when the bridge molecule is redox active and the formal oxidation–reduction potential of its redox moiety lies at a potential near or between the potentials of the two electrodes, as illustrated in **Figure 5c**. Under these conditions, so-called sequential tunneling can take place in which individual electrons hop from one electrode onto the molecule and reside in one of its well-defined electronic states for some time before finally hopping to the second electrode. In electrochemical terminology, this corresponds to the bridge molecule being reduced by the first electrode and subsequently oxidized by the second electrode, returning it to its initial state. This cycle is then repeated, each cycle transferring an electron from the first to the second electrode and inducing a steady current. More complex scenarios can also be envisaged in which tunneling via an electronic state of the bridge molecule is coherent instead of occurring in two independent steps, or in which relaxation of the molecule profoundly influences electron transport. These variants nonetheless share the basic feature that transport is enhanced when the potential of the electrodes is tuned to the vicinity of the formal potential of the redox moiety or, for large values of the applied potential ΔU , when the electrodes simultaneously have large reducing and oxidizing overpotentials.

The subfield of electrochemical single-molecule junctions was launched in a landmark 1996 paper by Tao (54), who employed an STM tip to image redox-active Fe(III)-protoporphyrin IX (FePP) molecules adsorbed in a regular lattice on a graphite surface (**Figure 6a**). Structurally similar, but redox-inactive, protoporphyrin IX (PP) molecules replacing FePP yielded much reduced apparent height in STM, corresponding to less efficient electron transport through the molecule (**Figure 6b**). The extra contrast, however, was observed only when the electrodes were biased close to the formal potential of FePP, indicating an electrochemical origin. Although the results were initially interpreted in terms of coherent tunneling, later analysis (55) supported the simpler sequential tunneling mechanism sketched in **Figure 5c**.

An important next step was the development by several laboratories of techniques for forming stable bridges across two electrodes (37, 39, 40, 43, 56). Mostly based on molecules incorporating thiol anchor groups for attachment to gold electrodes, these allowed systematic electron-transport measurements under controlled conditions on a wide array of both redox (38–41, 56) and nonredox (40, 43) molecules. A representative result is given in **Figure 6c**, which shows the current through 4,4'-bipyridine molecules bridging between an Au electrode and an Au STM tip while the tip

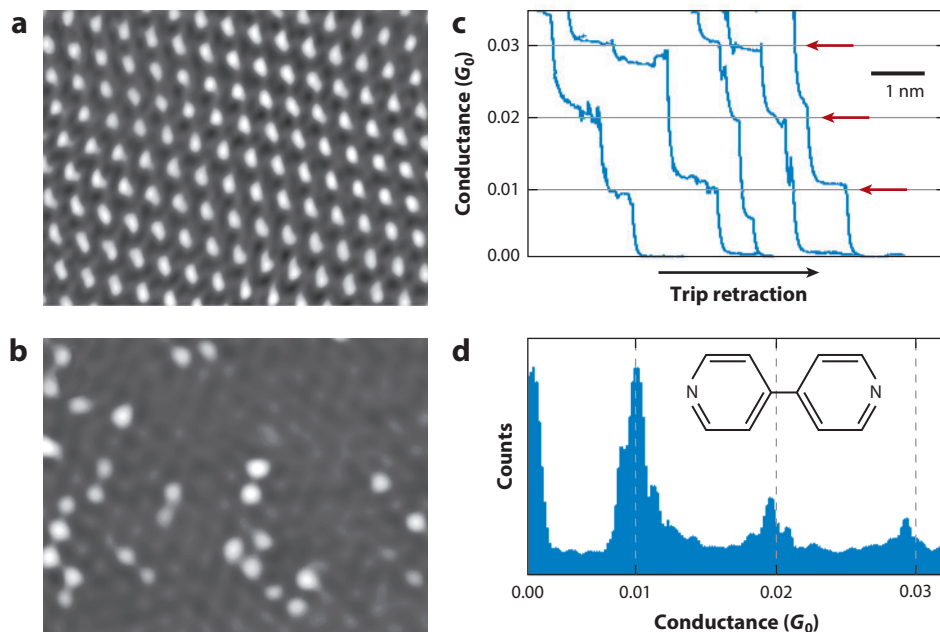


Figure 6

(*a,b*) Scanning tunneling microscopy (STM) image of a lattice of redox-active FePP molecules (*a*) and of FePP mixed with inactive protoporphyrin IX (PP) molecules. (*b*) Sequential tunneling through FePP leads to their higher apparent heights in panel *b*. Reproduced with permission from Reference 54. Copyright 1996 by the American Physical Society. (*c*) Current versus distance as an STM tip is retracted from a surface. Discrete jumps in the tunneling current correspond to individual 4,4'-bipyridine molecular bridges being broken. (*d*) Histogram of more than 1,000 measurements showing quantized conductance levels associated with individual molecular bridges. Reproduced from Reference 40 with permission of the Royal Society of Chemistry.

is being gradually retracted. Discrete steps in the current are observed in each of the four scans shown, each step being attributed to the breakage of a single-molecule contact. A histogram of the observed conductance values based on more than 1,000 retraction scans (reproduced in **Figure 6d**) shows discrete peaks corresponding to a conductance per molecule of $\sim 0.01 G_0$, where $G_0 = 77.4 \mu\text{S}$ corresponds to the so-called conductance quantum (40).

A further refinement of several molecular-junction approaches is the ability to obtain extensive statistics by repeated withdrawal and approach cycles (37, 39, 40, 42, 43). This has proven particularly crucial because of the high heterogeneity of single-molecule data and their dependence on molecular configuration (42, 57): measurements on hundreds or thousands of molecular junctions are often needed before a coherent picture emerges, as foreshadowed by **Figure 6d**. For example, even for small prototypical alkanedithiols (1,9-nonanedithiol) the bridge conductance can vary by one or more order of magnitude between molecules (57). Such pronounced variability was attributed to a strong dependence on subtle structural factors such as the coordination of the anchor sulfur atoms to the electrode atoms, illustrating a recurring theme in molecular electronic systems: a supreme sensitivity to details of molecular arrangement. But when probing these configurations statistically, impressively detailed information on the electronic transport of individual molecules can nonetheless be gleaned.

ELECTROCHEMICAL NANOFLUIDICS

Single-molecule electrochemical methods based on the trapping of single molecules between electrodes, as described in the previous section, have yielded major advances in our understanding of electron-transfer processes at the molecular level. From an analytical point of view, however, one is often interested in measuring species in solution without first needing to anchor them to a surface or electrodes. Developing assays capable of electrically detecting and characterizing individual molecules in a liquid sample is therefore highly desirable, albeit challenging, due to the small amount of charge transferred in individual electron-transfer events.

This obstacle can be overcome by amplifying the electrical signal generated by a single molecule by averaging over several oxidation or reduction events. Doing so requires a chemically reversible analyte that can be repeatedly reduced and oxidized, i.e., that can undergo redox cycling. Suitable analytes include important neurotransmitters and hormones such as dopamine and adrenaline, enzymes containing a redox-active cofactor such as FAD (58), and many broadly employed redox mediators such as ferricyanide $[\text{Fe}(\text{CN})_6]^{3-}$ or organometallic compounds (59). Conceptually, redox cycling closely resembles the sequential tunneling mechanism sketched in **Figure 5c**, the main difference being that the molecule must be transported between the electrodes before each step of the cycle is allowed to proceed. It follows that the resulting current levels are several orders of magnitude smaller than in the molecular junctions discussed above.

The most straightforward manner for achieving efficient and highly amplified redox cycling of a molecule in solution employs two electrodes positioned at a close distance from each other and biased at oxidizing and reducing overpotentials, respectively, as sketched in **Figure 7a**. Several approaches have been developed for creating this geometry, including positioning ultramicroelectrodes near a conducting surface using scanning electrochemical microscopy (SECM) (60, 61), interdigitated electrodes (62, 63), and thin-layer cells (64, 65). A key requirement is that the spacing between the electrodes should be much smaller than their lateral dimensions, such that a molecule entering the region between the electrodes by Brownian motion will cycle several times before it can wander off again.

All redox-cycling single-molecule experiments so far were performed at high supporting electrolyte concentrations; hence, mass transport was dominated by diffusion. Transport of ions could be further enhanced by migration if a strong electrical field was established between the electrodes (i.e., if no salt was used and the screening Debye double layer extended across the interelectrode distance), but such an experiment has yet to be realized. The average time t to perform a half cycle by diffusively crossing the distance L between two opposing electrodes is thus given by the classic result from Brownian motion theory, $t = L^2/2D$. This scales very favorably with the distance L , highlighting why it is crucial to reduce the interelectrode spacing to achieve measurable single-molecule signals. For a diffusion coefficient $D = 5 \times 10^{-10} \text{ m}^2\text{s}^{-1}$ (typical for standard organometallic redox compounds such as ferrocenes in aqueous solution) and an electrode spacing $L = 50 \text{ nm}$, the average transit across the interelectrode distance thus takes $2.5 \mu\text{s}$. The corresponding theoretical value for the single-molecule current is given by (68)

$$i_0 = \frac{enD}{L^2}, \quad 1.$$

where $-e$ is the electron charge and n is the number of electrons transferred. For the parameters above, i_0 amounts to 30 fA for a single-ET reaction (see sidebar, Limits of Electrical Instrumentation). This is, however, only an idealized upper bound obtained by assuming infinite, homogenous parallel plate electrodes, instantaneous ET at the electrodes, and no adsorption.

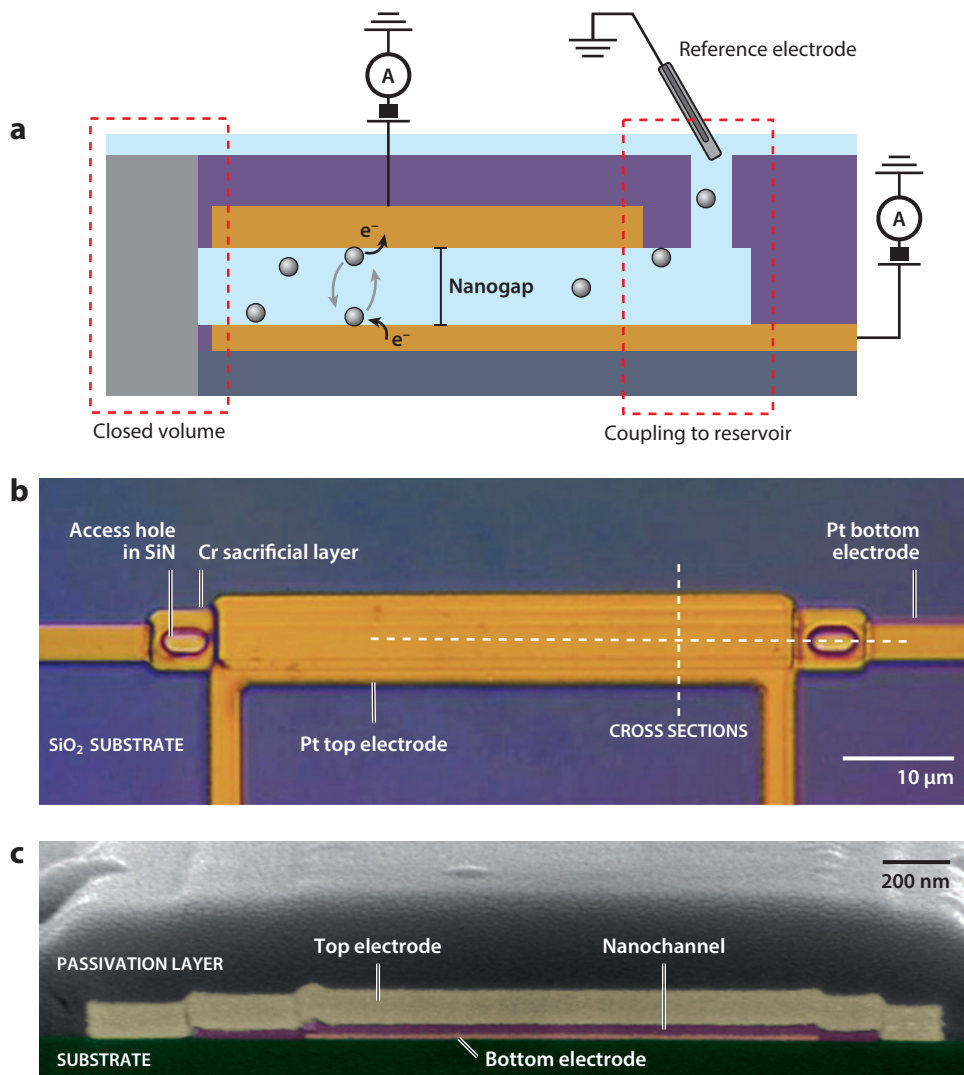


Figure 7

(a) Schematic cross section of a redox-cycling transducer. Redox-active molecules diffuse between the closely spaced (<100 nm) electrodes, where they are repeatedly oxidized and reduced to generate a highly amplified electrochemical current. The liquid volume between the electrodes can be either closed [e.g., by a (left) wax or polymer sheath surrounding an electrode tip] or coupled to a larger reservoir in the case of fixed-geometry microfabricated sensors (right). (b) Optical micrograph (top) of a nanogap device consisting of a $50\text{-}\mu\text{m}$ -long and $5\text{-}\mu\text{m}$ -wide detection region. The solution-filled nanochannel is originally defined by a sacrificial Cr layer, which is etched immediately prior to electrochemical measurements. The horizontal and vertical dashed lines correspond to the schematic cross section in panel a and the micrograph in panel c, respectively. (c) Scanning-electron micrograph of the lateral cross section of a nanogap device cut open by a focused ion beam. Panels a and b adapted from Reference 66, copyright 2013 by Elsevier. Panel c from Reference 67, Copyright © (2011) American Chemical Society.

LIMITS OF ELECTRICAL INSTRUMENTATION

Measuring the small electrical currents associated with single-molecule redox cycling can represent a significant experimental challenge. Commercial ultralow-noise transimpedance amplifiers based on op amp circuitry (a typical example at the time of writing being the DDPCA-300 from FEMTO) can exhibit noise as low as 1 fA peak to peak when the input is open-circuited (with a corresponding response time of ~ 100 ms). Upon connection to an electrode in solution, however, the noise level can easily increase by an order of magnitude or more. This is primarily due to the capacitance of the electrode and its associated interconnects, which converts the amplifier's input voltage noise into a current noise that is then amplified together with the real signal.

To detect a single molecule, Fan and Bard (68, 69) employed redox cycling at closely spaced electrodes in 1995. They used a scanning electrochemical microscope configuration to trap a small number of [(trimethylammonio)methyl]ferrocene molecules between a Pt-Ir tip and an ITO ultramicroelectrode. A wax sheath was employed to localize analyte molecules in the detection region immediately below the electrode. Reducing the electrode distance down to 10 nm, they observed discrete current fluctuations of approximately 700 fA, as shown in **Figure 8a**. These fluctuations were attributed to individual molecules entering and leaving the detection region between the electrodes as a result of the molecules being occasionally trapped in the wax sheath.

This approach was further explored by Sun & Mirkin (70), who immersed a recessed nanoelectrode first in an aqueous solution containing ferrocenemethanol and successively in a Hg bath. Their observations were consistent with the assumption that a small volume of water became trapped between the electrode and the Hg bath, thus forming a nanogap geometry. At very low concentrations, variations in the redox-cycling current between successive experiments with the same electrode were attributed to statistical fluctuations in the number of molecules trapped in the detection volume. On the basis of this interpretation, measurements on a 7-nm-thin cavity yielded a current per molecule of 2 pA.

Although it was possible to capitalize on SECM technology for the first exploratory attempts at single-molecule measurements, limitations of the approach seem to have prevented further studies. In particular, the inherent challenge in fabricating tip-based nanoelectrodes with a verifiable, reproducible geometry has precluded systematic measurements. Varying tip sizes and interelectrode distances preclude achieving equivalent conditions between experiments and reproducible, controlled transport of analyte molecules into the detection region. For extensive measurements, a more controlled and highly reproducible environment and geometry are therefore highly desirable. The foundations for such a geometry were introduced first in 1965 in the form of thin-layer cells consisting of well-defined planar electrodes defining the floor and roof of a fluidic channel (64, 71). Recently, this concept was further optimized using modern microfabrication technology to manufacture nanoscale thin-layer cells—or nanogaps for short—that permit reaching single-molecule sensitivity (65).

Nanogap sensors consist of two metal electrodes embedded in the floor and ceiling of a nanofluidic channel, as shown in **Figure 7b,c**. Hundreds of devices can be fabricated simultaneously on a silicon wafer substrate using photolithographic microfabrication (72), and the critical interelectrode distance is defined reliably by the thickness of an evaporated sacrificial Cr layer (66, 72).

Single-molecule sensing in nanogap sensors was demonstrated in 2011 by the detection of ferrocene molecules in acetonitrile at Pt electrodes separated by a 70-nm gap (67). Individual molecules could diffuse between the detection region and an external reservoir, yielding a

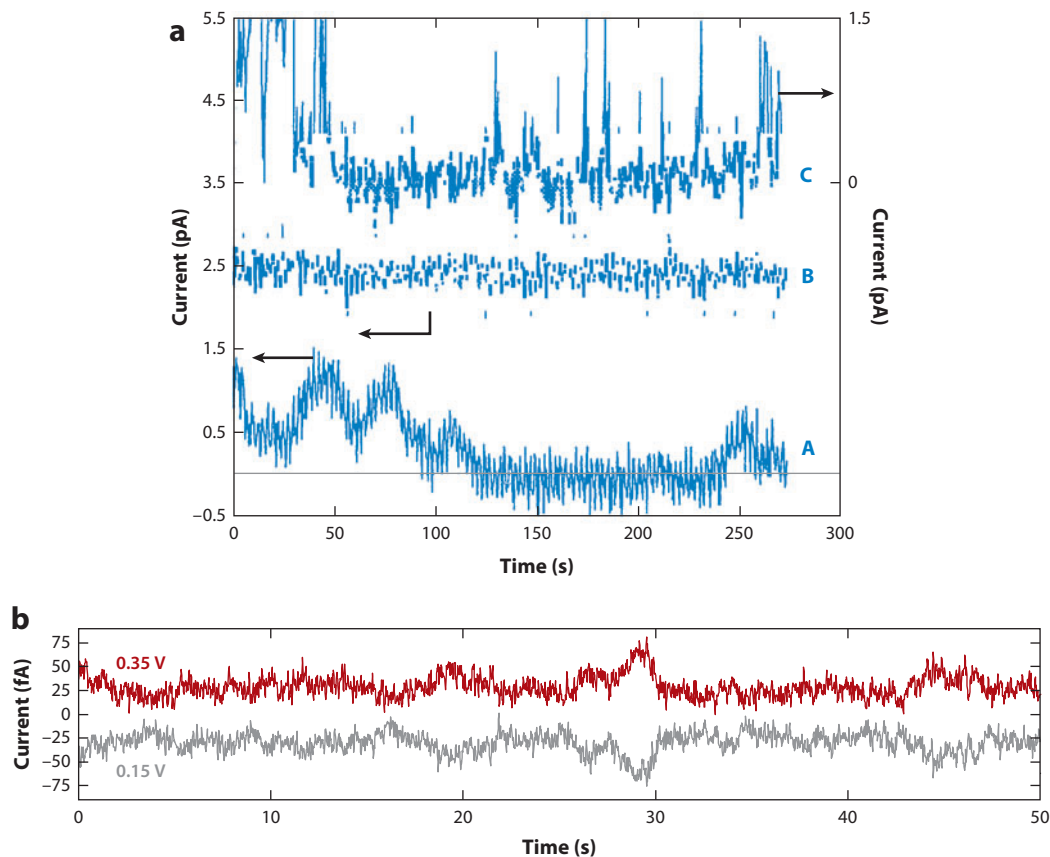


Figure 8

Stochastic sensing. (a) Current-time traces at a Pt-Ir electrode tip at a potential of 0.85 V versus an indium tin oxide substrate (two-electrode configuration). Curve A shows a measurement of $\text{Cp}_2\text{FeTMA}^+$ in aqueous solution with NaNO_3 as the supporting electrolyte. The curve reaches peaks of 0.7 pA and 1.4 pA, which were interpreted as one and two molecules being trapped between tip and surface (curve B: control experiment showing the background current at a large tip-substrate distance; curve C: control experiment depicting the current in the absence of $\text{Cp}_2\text{FeTMA}^+$ at a short tunneling distance). From Reference 68, © The American Association for the Advancement of Science. (b) Current-time traces recorded at the top and bottom Pt electrodes of a nanogap sensor with a 70-nm gap size. Ferrocene molecules are detected in a 120-pM solution in acetonitrile at biases of 0.35 V (*top electrode*) and -0.15 V (*bottom electrode*) versus Ag/AgNO_3 in a monovalent salt. Redox-active molecules generate identical currents—but with reversed polarity—at the opposing electrodes, thus making it possible to distinguish the faradaic current from parasitic noise. A current level of 20 fA is attributed to a single ferrocene molecule being present in the nanogap. From Reference 67, Copyright © (2011) American Chemical Society.

current while residing in the detection region. Single-molecule events could be separated from the background instrumental noise by simultaneously measuring the current through both electrodes, redox cycling yielding identical current-time responses with reversed polarities at the two electrodes. A measurement from Reference 67 is shown in **Figure 8b** for illustration. Single molecules yielded a current of 20 fA at each electrode, corresponding to a signal-to-noise ratio of ~ 1 .

A significant discrepancy between the three reports of single-molecule amperometric detection to date pertains to the magnitude of the single-molecule current. Whereas References 68 and 70 reported current levels consistent with pure diffusion, as predicted by Equation 1, the results in

Reference 67 exhibited a suppression of the signal by a factor of ~ 4 compared to this prediction. The suppression was attributed to reversible adsorption of the analyte at the surfaces of the electrodes. Adsorption of outer-sphere reactants, which do not require a covalent bridge for ET, typically does not influence macro- and microscale measurements, given that submonolayer coverage has negligible impact on mass transport. At the extremely high surface-to-volume ratios of nanochannels of 10^7 m^{-1} or larger, however, the role of any residual adsorption is greatly magnified. Measurements in nanogap devices at high concentration indeed find pronounced signatures of adsorption, with the degree of adsorption corresponding to each molecule spending a factor of 2–4 more time adsorbed to the electrodes than freely diffusing (66, 73–75), consistent with the observed suppression of the single-molecule current in Reference 67. A consequence of this interpretation is that at an electrode spacing of $\sim 100 \text{ nm}$ or less, adsorption becomes the dominant factor slowing down the rate at which a molecule can undergo redox cycling. In our view, the development of an understanding of the mechanism of this reversible adsorption will be a key step in single-molecule redox cycling, as it could lead to a reconciliation with the earlier experiments (68–70), in which no adsorption was reported. Moreover, new ways of reducing adsorption could allow for more reliable detection of single molecules with an improved signal-to-noise ratio.

So far, single molecules have been sensed stochastically: A random number of molecules was trapped in the detection volume (70), or the detection volume was coupled to a reservoir from which molecules could enter at random times by diffusion (65, 68). When coupled to a reservoir, however, the residence time of single molecules is statistically distributed over a wide range of timescales (69, 76). One consequence is that only rare, particularly long single-molecule events can be resolved; shorter events are simply averaged out by the necessarily limited time resolution of the measurement electronics. We propose that this limitation can be overcome in future experiments by driving a convective flow through the nanogap sensor. When liquid is pumped fast enough, the advection of analyte molecules dominates diffusive transport along the nanochannel. The residence time in the active region of the sensor is then directly controlled, i.e., all molecules traverse the channel in approximately the same time and should be detected as similar-duration events, as supported by simulations (76, 77).

Additional possibilities also open when pressure-driven flow is combined with multiple nanogap transducers in a single nanochannel, a system that some of us have recently employed as a sensitive flow meter (66, 78). Several subsequent electrode pairs could either improve the reliability of detection if a single molecule is measured repeatedly as it passes along the nanochannel. Alternatively, biasing the electrodes at different potentials matched to different analytes would allow fingerprinting individual molecules as they travel through the system.

CONCLUSIONS AND OUTLOOK

As the work reviewed here shows, various methods based on several distinct signal-transduction mechanisms have been developed to allow probing electrochemical phenomena at the level of single molecules. Optical techniques offer several advantages compared to conventional electrochemical approaches, especially with regard to sensitivity. The fluorescent labeling method for studying redox proteins and enzymes in particular stands out because of its relative simplicity and generic character and because it does not interfere with their natural function. There are additional good reasons for combining electrochemistry with optical detection. These include, for example, the ability to help understand the (still ill-characterized) interaction between solid surfaces and immobilized (bio)molecules; the acquisition of complementary information to help elucidate the internal workings of complex multicentered oxidoreductase enzymes; and the ability to explore the redox behavior of electroactive materials used in solid-state devices such as photovoltaic cells,

light-emitting diodes, and organic transistors. Efforts so far have primarily focused on showing that the combination of the two techniques is feasible. Apart from a few examples, the investigation of detailed optical (fluorescence) time traces has still remained largely unexplored and will likely prove to be a rich source of further information.

Methods based on electrical detection instead have the advantage of providing direct electrochemical information, thus facilitating quantitative interpretation and establishing links to more conventional macroscopic measurements. Indeed, molecular junctions so far represent the single-molecule approach that has yielded the most detailed information on electron-transfer mechanisms. In comparison, detection based on redox cycling has the advantage that molecules can be detected directly in solution without prior immobilization, but practical implementation remains challenging and limited by stochastic fluctuations. Approaches being introduced to control mass transport and thus mitigate the randomness inherent to diffusion have in our view the potential to greatly broaden the range of applicability of single-molecule electrochemical methods.

SUMMARY POINTS

1. Electrochemistry provides a transduction mechanism that has not yet been widely exploited in single-molecule experiments.
2. Redox proteins and enzymes can be fluorescently labeled to monitor their redox state and associated ET reactions at the single-molecule level. When immobilized on a transparent electrode, electrochemically induced redox changes in these systems can be measured with unmatched sensitivity.
3. This (generic) method of fluorescent labeling provides access to measuring the heterogeneity of redox parameters of proteins and enzymes, e.g., midpoint potential and interfacial ET rates, by optical detection at the microscopic and single-molecule level.
4. The tunneling current between two electrodes bridged by a single redox molecule acts as a probe of the redox state of the molecule. The current is very sensitive to the exact molecular arrangement, often necessitating the acquisition of large data sets for quantitative analysis.
5. Single molecules in solution can be detected via redox cycling between two electrodes with nanometer-scale spacing. This detection necessarily averages over several oxidation/reduction cycles.

FUTURE ISSUES

1. Can fluorescence-detected CV of a single, fluorescently labeled redox protein or enzyme be achieved?
2. Can ET between a donor and an acceptor, both consisting of suitably labeled redox proteins (e.g., an enzyme and its reaction partner), be monitored in a single reaction complex with one of the components (or both, as in Reference 79) being localized on an electrode under potentiostatic control?
3. Can molecular junctions be created with a sufficient level of atomic-scale control that measurements become reproducible between molecules?

4. Can the reversible adsorption of redox molecules to electrodes be sufficiently suppressed that it no longer limits the observed single-molecule current in redox cycling?
5. Can single-molecule electrochemical fingerprinting lead to new or improved analytical techniques applicable to complex mixtures of redox-active species?

DISCLOSURE STATEMENT

The authors are not aware of any affiliations, memberships, funding, or financial holdings that might be perceived as affecting the objectivity of this review.

ACKNOWLEDGMENTS

K.M. and S.G.L. gratefully acknowledge financial support from the Netherlands Organization for Scientific Research (NWO), the European Research Council (ERC) and the Semiconductor Research Corporation (SRC). The work by T.J.A. and G.W.C. is part of the research program of the Foundation for Fundamental Research on Matter (FOM) and of the Chemical Sciences TOP program, both of which are (partly) financed by the NWO. They also acknowledge support by the European Commission through the EdRox Network (contract no. MRTN-CT-2006-035649).

LITERATURE CITED

1. Walter NG, Huang C-Y, Manzo AJ, Sobhy MA. 2008. Do-it-yourself guide: how to use the modern single-molecule toolkit. *Nat. Methods* 5:475–89
2. Shon MJ, Cohen AE. 2012. Mass action at the single-molecule level. *J. Am. Chem. Soc.* 134:14618–23
3. Eid J, Fehr A, Gray J, Luong K, Lyle J, et al. 2009. Real-time DNA sequencing from single polymerase molecules. *Science* 323:133–38
4. Kwon SJ, Zhou H, Fan F-RF, Vorobyev V, Zhang B, Bard AJ. 2011. Stochastic electrochemistry with electrocatalytic nanoparticles at inert ultramicroelectrodes—theory and experiments. *Phys. Chem. Chem. Phys.* 13:5394–402
5. Xiao X, Bard AJ. 2007. Observing single nanoparticle collisions at an ultramicroelectrode by electrocatalytic amplification. *J. Am. Chem. Soc.* 129:9610–12
6. Xiao X, Fan F-RF, Zhou J, Bard AJ. 2008. Current transients in single nanoparticle collision events. *J. Am. Chem. Soc.* 130:16669–77
7. Kleijn SEF, Lai SCS, Miller TS, Yanson AI, Koper MTM, Unwin PR. 2012. Landing and catalytic characterization of individual nanoparticles on electrode surfaces. *J. Am. Chem. Soc.* 134:18558–61
8. Shan X, Diez-Perez I, Wang L, Wiktor P, Gu Y, et al. 2012. Imaging the electrocatalytic activity of single nanoparticles. *Nat. Nanotechnol.* 7:668–72
9. Armstrong FA, Heering HA, Hirst J. 1997. Reactions of complex metalloproteins studied by protein-film voltammetry. *Chem. Soc. Rev.* 26:169–79
10. Bernhardt PV. 2006. Enzyme electrochemistry—biocatalysis on an electrode. *Aust. J. Chem.* 59:233–56
11. Hoeben FJM, Meijer FS, Dekker C, Albracht SPJ, Heering HA, Lemay SG. 2008. Toward single-enzyme molecule electrochemistry: [NiFe]-hydrogenase protein film voltammetry at nanoelectrodes. *ACS Nano* 2:2497–504
12. Audebert P, Miomandre F. 2013. Electrofluorochromism: from molecular systems to set-up and display. *Chem. Sci.* 4:575–84
13. Lei CH, Hu DH, Ackerman EJ. 2008. Single-molecule fluorescence spectroelectrochemistry of cresyl violet. *Chem. Commun.* 2008:5490–92
14. Lei CH, Hu DH, Ackerman E. 2009. Clay nanoparticle-supported single-molecule fluorescence spectroelectrochemistry. *Nano Lett.* 9:655–58

26. Illustrates new information that can be gleaned from single-molecule studies of fluorescently labeled enzymes.

28. The first study in which heterogeneous electrochemistry is combined with optical detection.

33. Elegant study of electron exchange between metallic Ag nanoparticles and immobilized hemin molecules.

34. Demonstrates single-molecule catalysis on carbon nanotubes and derives detailed information on catalytic activity.

15. Yang SK, Shi X, Park S, Ha T, Zimmerman SC. 2013. A dendritic single-molecule fluorescent probe that is monovalent, photostable and minimally blinking. *Nat. Chem.* 5:692–97
16. Zhao J, Zaino LP 3rd, Bohn PW. 2013. Potential-dependent single molecule blinking dynamics for flavin adenine dinucleotide covalently immobilized in zero-mode waveguide array of working electrodes. *Faraday Discuss.* 164:57–69
17. Palacios RE, Fan FRF, Bard AJ, Barbara PF. 2006. Single-molecule spectroelectrochemistry (SMS-EC). *J. Am. Chem. Soc.* 128:9028–29
18. Palacios RE, Fan FRF, Grey JK, Suk J, Bard AJ, Barbara PF. 2007. Charging and discharging of single conjugated-polymer nanoparticles. *Nat. Mater.* 6:680–85
19. Zhang GF, Xiao LT, Chen RY, Gao Y, Wang XB, Jia ST. 2011. Single-molecule interfacial electron transfer dynamics manipulated by an external electric current. *Phys. Chem. Chem. Phys.* 13:13815–20
20. Chang Y-L, Palacios RE, Fan F-RF, Bard AJ, Barbara PF. 2008. Electrogenerated chemiluminescence of single conjugated polymer nanoparticles. *J. Am. Chem. Soc.* 130:8906–7
21. Vijgenboom E, Busch JE, Canters GW. 1997. *In vivo* studies disprove an obligatory role of azurin in denitrification in *Pseudomonas aeruginosa* and show that *azu* expression is under control of RpoS and ANR. *Microbiology* 143:2853–63
22. Kuznetsova S, Zauner G, Schmauder R, Mayboroda OA, Deelder AM, et al. 2006. A Forster-resonance-energy transfer-based method for fluorescence detection of the protein redox state. *Anal. Biochem.* 350:52–60
23. Schmauder R, Librizzi F, Canters GW, Schmidt T, Aartsma TJ. 2005. The oxidation state of a protein observed molecule-by-molecule. *Chemphyschem* 6:1381–86
24. Goldsmith RH, Tabares LC, Kostrz D, Dennison C, Aartsma TJ, et al. 2011. Redox cycling and kinetic analysis of single molecules of solution-phase nitrite reductase. *Proc. Natl. Acad. Sci. USA* 108:17269–74
25. Kuznetsova S, Zauner G, Aartsma TJ, Engelkamp H, Hatzakis N, et al. 2008. The enzyme mechanism of nitrite reductase studied at single-molecule level. *Proc. Natl. Acad. Sci. USA* 105:3250–55
26. Tabares LC, Kostrz D, Elmalk A, Andreoni A, Dennison C, et al. 2011. Fluorescence lifetime analysis of nitrite reductase from *Alcaligenes xylosoxidans* at the single-molecule level reveals the enzyme mechanism. *Chem.-Eur. J.* 17:12015–19
27. Davis JJ, Burgess H, Zauner G, Kuznetsova S, Salverda J, et al. 2006. Monitoring interfacial bioelectrochemistry using a FRET switch. *J. Phys. Chem. B* 110:20649–54
28. Salverda JM, Patil AV, Mizzon G, Kuznetsova S, Zauner G, et al. 2010. Fluorescent cyclic voltammetry of immobilized azurin: direct observation of thermodynamic and kinetic heterogeneity. *Angew. Chem.-Int. Ed.* 49:5776–79
29. Patil AV, Davis JJ. 2010. Visualizing and tuning thermodynamic dispersion in metalloprotein monolayers. *J. Am. Chem. Soc.* 132:16938–44
30. Cortés E, Etchegoin PG, Le Ru EC, Fainstein A, Vela ME, Salvarezza RC. 2010. Monitoring the electrochemistry of single molecules by surface-enhanced Raman spectroscopy. *J. Am. Chem. Soc.* 132:18034–37
31. van de Linde S, Sauer M. 2014. How to switch a fluorophore: from undesired blinking to controlled photoswitching. *Chem. Soc. Rev.* 43:1076–87
32. Pu K, Shuhendler AJ, Rao J. 2013. Semiconducting polymer nanoprobe for in vivo imaging of reactive oxygen and nitrogen species. *Angew. Chem.* 52:10325–29
33. Wang YM, Sevinc PC, He YF, Lu HP. 2011. Probing ground-state single-electron self-exchange across a molecule-metal interface. *J. Am. Chem. Soc.* 133:6989–96
34. Shen H, Xu WL, Chen P. 2010. Single-molecule nanoscale electrocatalysis. *Phys. Chem. Chem. Phys.* 12:6555–63
35. Bard AJ, Faulkner LR. 2000. *Electrochemical Methods: Fundamentals and Applications*. New York: Wiley
36. McCreery RL, Bergren AJ. 2009. Progress with molecular electronic junctions: meeting experimental challenges in design and fabrication. *Adv. Mater.* 21:4303–22
37. Xu BQ, Tao NJJ. 2003. Measurement of single-molecule resistance by repeated formation of molecular junctions. *Science* 301:1221–23
38. Li Z, Han B, Meszaros G, Pobelov I, Wandlowski T, et al. 2006. Two-dimensional assembly and local redox-activity of molecular hybrid structures in an electrochemical environment. *Faraday Discuss.* 131:121–43

39. Haiss W, van Zalinge H, Higgins SJ, Bethell D, Hobenreich H, et al. 2003. Redox state dependence of single molecule conductivity. *J. Am. Chem. Soc.* 125:15294–95
40. Li XL, Xu BQ, Xiao XY, Yang XM, Zang L, Tao NJ. 2006. Controlling charge transport in single molecules using electrochemical gate. *Faraday Discuss.* 131:111–20
41. He J, Fu Q, Lindsay S, Ciszek JW, Tour JM. 2006. Electrochemical origin of voltage-controlled molecular conductance switching. *J. Am. Chem. Soc.* 128:14828–35
42. Chen F, Nuckolls C, Lindsay S. 2006. In situ measurements of oligoaniline conductance: linking electrochemistry and molecular electronics. *Chem. Phys.* 324:236–43
43. Haiss W, Nichols RJ, van Zalinge H, Higgins SJ, Bethell D, Schiffrin DJ. 2004. Measurement of single molecule conductivity using the spontaneous formation of molecular wires. *Phys. Chem. Chem. Phys.* 6:4330–37
44. Cui XD, Primak A, Zarate X, Tomfohr J, Sankey OF, et al. 2001. Reproducible measurement of single-molecule conductivity. *Science* 294:571–74
45. Boussaad S, Tao NJ. 2002. Atom-size gaps and contacts between electrodes fabricated with a self-terminated electrochemical method. *Appl. Phys. Lett.* 80:2398–400
46. Xiang J, Liu B, Wu ST, Ren B, Yang FZ, et al. 2005. A controllable electrochemical fabrication of metallic electrodes with a nanometer/angstrom-sized gap using an electric double layer as feedback. *Angew. Chem.* 44:1265–68
47. Tian JH, Liu B, Li XL, Yang ZL, Ren B, et al. 2006. Study of molecular junctions with a combined surface-enhanced Raman and mechanically controllable break junction method. *J. Am. Chem. Soc.* 128:14748–49
48. Zhang J, Kuznetsov AM, Medvedev IG, Chi Q, Albrecht T, et al. 2008. Single-molecule electron transfer in electrochemical environments. *Chem. Rev.* 108:2737–91
49. Zhang JD, Chi QJ, Hansen AG, Jensen PS, Salvatore P, Ulstrup J. 2012. Interfacial electrochemical electron transfer in biology—towards the level of the single molecule. *FEBS Lett.* 586:526–35
50. Li C, Mishchenko A, Pobelov I, Wandlowski T. 2010. Charge transport with single molecules—an electrochemical approach. *Chimia* 64:383–90
51. Nichols RJ, Haiss W, Higgins SJ, Leary E, Martin S, Bethell D. 2010. The experimental determination of the conductance of single molecules. *Phys. Chem. Chem. Phys.* 12:2801–15
52. Chen F, Tao NJ. 2009. Electron transport in single molecules: from benzene to graphene. *Acc. Chem. Res.* 42:429–38
53. Chen F, Hihath J, Huang ZF, Li XL, Tao NJ. 2007. Measurement of single-molecule conductance. *Annu. Rev. Phys. Chem.* 58:535–64
- 54. Tao NJ. 1996. Probing potential-tuned resonant tunneling through redox molecules with scanning tunneling microscopy. *Phys. Rev. Lett.* 76:4066–69**
55. Kuznetsov AM, Ulstrup J. 2000. Mechanisms of in situ scanning tunnelling microscopy of organized redox molecular assemblies. *J. Phys. Chem. A* 104:11531–40
56. Chen F, He J, Nuckolls C, Roberts T, Klare JE, Lindsay S. 2005. A molecular switch based on potential-induced changes of oxidation state. *Nano Lett.* 5:503–6
57. Li C, Pobelov I, Wandlowski T, Bagrets A, Arnold A, Evers F. 2008. Charge transport in single Au | alkanedithiol | Au junctions: coordination geometries and conformational degrees of freedom. *J. Am. Chem. Soc.* 130:318–26
58. Gorton L, Johansson G. 1980. Cyclic voltammetry of FAD adsorbed on graphite, glassy carbon, platinum and gold electrodes. *J. Electroanal. Chem. Interfacial Electrochem.* 113:151–58
59. Connelly NG, Geiger WE. 1996. Chemical redox agents for organometallic chemistry. *Chem. Rev.* 96:877–910
60. Engstrom RC, Weber M, Wunder DJ, Burgess R, Winquist S. 1986. Measurements within the diffusion layer using a microelectrode probe. *Anal. Chem.* 58:844–48
61. Bard AJ, Mirkin MV, eds. 2012. *Scanning Electrochemical Microscopy*. Boca Raton, Fla., CRC. 2nd ed.
62. Sanderson DG, Anderson LB. 1985. Filare electrodes: steady-state currents and spectroelectrochemistry at twin interdigitated electrodes. *Anal. Chem.* 57:2388–93
63. Goluch ED, Wolfrum B, Singh PS, Zevenbergen MA, Lemay SG. 2009. Redox cycling in nanofluidic channels using interdigitated electrodes. *Anal. Bioanal. Chem.* 394:447–56

54. Landmark experiment on addressing individual redox-active molecules under potential control using an STM.

67. First study of single-molecule detection by redox cycling in a microfabricated device.

68. The first report on amperometric single-molecule detection.

64. Anderson LB, Reilley CN. 1965. Thin-layer electrochemistry: use of twin working electrodes for the study of chemical kinetics. *J. Electroanal. Chem.* 1959 10:538–52
65. Zevenbergen MA, Krapf D, Zuiddam MR, Lemay SG. 2007. Mesoscopic concentration fluctuations in a fluidic nanocavity detected by redox cycling. *Nano Lett.* 7:384–88
66. Mathwig K, Lemay SG. 2013. Pushing the limits of electrical detection of ultralow flows in nanofluidic channels. *Micromachines* 4:138–48
67. Zevenbergen MA, Singh PS, Goluch ED, Wolfrum BL, Lemay SG. 2011. Stochastic sensing of single molecules in a nanofluidic electrochemical device. *Nano Lett.* 11:2881–86
68. Fan F-RF, Bard AJ. 1995. Electrochemical detection of single molecules. *Science* 267:871–74
69. Bard AJ, Fan F-RF. 1996. Electrochemical detection of single molecules. *Acc. Chem. Res.* 29:572–78
70. Sun P, Mirkin MV. 2008. Electrochemistry of individual molecules in zeptoliter volumes. *J. Am. Chem. Soc.* 130:8241–50
71. Anderson LB, Reilley CN. 1965. Thin-layer electrochemistry: steady-state methods of studying rate processes. *J. Electroanal. Chem.* 1959 10:295–305
72. Rassaei L, Singh PS, Lemay SG. 2011. Lithography-based nanoelectrochemistry. *Anal. Chem.* 83:3974–80
73. Mathwig K, Lemay SG. 2013. Mass transport in electrochemical nanogap sensors. *Electrochim. Acta* 112:943–49
74. Singh PS, Chan HSM, Kang S, Lemay SG. 2011. Stochastic amperometric fluctuations as a probe for dynamic adsorption in nanofluidic electrochemical systems. *J. Am. Chem. Soc.* 133:18289–95
75. Kang S, Mathwig K, Lemay SG. 2012. Response time of nanofluidic electrochemical sensors. *Lab Chip* 12:1262–67
76. Singh PS, Kätelhön E, Mathwig K, Wolfrum B, Lemay SG. 2012. Stochasticity in single-molecule nanoelectrochemistry: origins, consequences, and solutions. *ACS Nano* 6:9662–71
77. Lemay SG, Kang S, Mathwig K, Singh PS. 2012. Single-molecule electrochemistry: present status and outlook. *Acc. Chem. Res.* 46:369–77
78. Mathwig K, Mampallil D, Kang S, Lemay SG. 2012. Electrical cross-correlation spectroscopy: measuring picoliter-per-minute flows in nanochannels. *Phys. Rev. Lett.* 109:118302
79. Tepper AW. 2010. Electrical contacting of an assembly of pseudoazurin and nitrite reductase using DNA-directed immobilization. *J. Am. Chem. Soc.* 132:6550–57